

## **SENSOR MODELING FOR AN ELECTRICAL CAPACITANCE TOMOGRAPHY SYSTEM USING COMSOL MULTIPHYSICS**

MUHAMMAD AFIQ ZIMAM<sup>1</sup>, ELMY JOHANA MOHAMAD<sup>2\*</sup>,  
RUZAIRI ABDUL RAHIM<sup>3</sup> & LEOW PEI LING<sup>4</sup>

**Abstract.** This work presents the development process for modeling an ECT (Electrical Capacitance Tomography) sensor using FEM software package COMSOL Multiphysics. The physical sensors are 3D dimensional but it has been common to model the slice or the cross-section in 2D. This project shows the modeling approach for 2D and 3D geometries, the linear Finite Element method (FEM) using COMSOL Multiphysics is developed in order to obtain the capacitance between electrodes when an electric field is applied and to obtain the permittivity distribution inside the closed pipe from the sensor. Generated phantoms and measured values are presented for empty and annular pattern. Simulation is verified using phantoms inside the 16 electrode sensor. The ECT model is representative by existing hardware, Portable ECT, PROTOM Research Group UTM.

*Keywords:* Sensor; modeling; ECT; COMSOL multiphysics

**Abstrak.** Kerja penyelidikan ini membentangkan proses pembinaan model bagi Pengesan Kapasitan Elektrik Tomografi (ECT) menggunakan Perisian Kaedah Elemen Terhingga (*Finite Element method FEM*) *COMSOL Multiphysics*. Meskipun pengesan fizikal adalah dalam bentuk tiga dimensi (3D) tetapi secara amnya sering dimodelkan secara kepingan/ keratan rentas dalam bentuk dua dimensi (2D). Projek ini menunjukkan pendekatan model dalam bentuk geometri 3D dan 2D, linear *FEM* menggunakan perisian *COMSOL Multiphysics* dibina adalah untuk mendapatkan nilai kapasitor di antara elektrod apabila medan elektrik dikenakan dan untuk melihat bagaimana pengagihan permittivity di dalam paip yang bertutup menerusi pengesan. Bayang-bayang yang direkapipta dan nilai-nilai diukur dikemukakan dalam bentuk paip yg kosong dan aliran anulus. Model ECT adalah mewakili perkakasan yang sedia ada, ECT mudah alih yang telah dibina oleh Kumpulan Penyelidikan PROTOM UTM.

*Kata kunci:* Pengesan; model; ECT; COMSOL multiphysics

---

<sup>1,3&4</sup> Process Tomography & Instrumentation Research Group, Cybernetics Research Alliance , Faculty of Electrical Engineering, Universiti Teknologi Malaysia, 81310 UTM Johor Bahru

<sup>2</sup> Department of Mechatronics and Robotics Engineering, Faculty of Electrical Electronics Engineering, Universiti Tun Hussein Onn Malaysia, 86400, Pt. Raja, Batu Pahat, Johor

\* Corresponding author: [elmy@uthm.edu.my](mailto:elmy@uthm.edu.my)

## 1.0 INTRODUCTION

This work concentrates on designing an ECT system with portable and mobile ability, thus external electrodes must be chosen instead of internal electrodes. Figure 1, illustrates an ECT system where the ECT sensor consists of sixteen electrodes mounted equidistantly along the periphery of an insulated pipe vessel.

The 16 segmented electrodes are numbered from 1 to 16, and the measurement protocol in the sensing electronics first measures the inter-electrode capacitance between electrodes one and two, then between one and three, and up to one and  $N$ , where  $N = 16$  in this case. Then, the capacitances between electrodes two and three, and up to two and  $N$  are measured. The measurements continue until all the inter-electrode capacitances are measured.

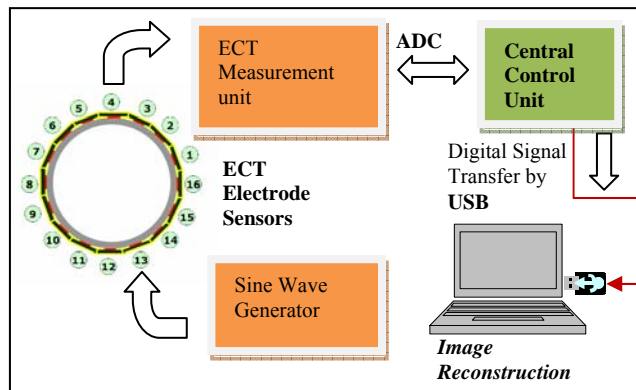


**Figure 1** ECT system topology

## 2.0 SENSOR MODELING

The first step to develop the numerical modeling is by drawing the shape of a pipeline which is a circle with a certain diameter. For this case, the drawing geometry used will follow the hardware actual size and geometry. Then alteration of the number of electrodes around the pipeline can be easily built.

The relationship between capacitance and dielectric properties can be given as follows: in any two adjacent conductors can be considering as a capacitor, and different dielectric properties between the conductors will create different

capacitor value as in (1), the sensors usually consist of two electrode plates and the capacitance. The measurement is determined by:

$$C = \frac{\epsilon_0 \epsilon_r A}{d_p} \quad (1)$$

Where

$C$  = capacitance (F)

$\epsilon_0$  = permittivity of free space

$\epsilon_r$  = permittivity of the dielectric

$A$  = area of the plate

$d_p$  = the distance between those plates

The  $\epsilon_0$  and  $\epsilon_r$  are the global average of the fluid dielectric property over the entire sensing volume of the sensor or better known as permittivity [1]. If the area of the plate and the distance between them are known, by measuring the capacitance; we are effectively measuring the dielectric constant. In this case, capacitance value is thus proportional to the permittivity in between the electrodes.

## 2.1 Modeling Process Using COMSOL Multiphysics

The design process for 16 portable electrode sensor models can be divided into following approach:

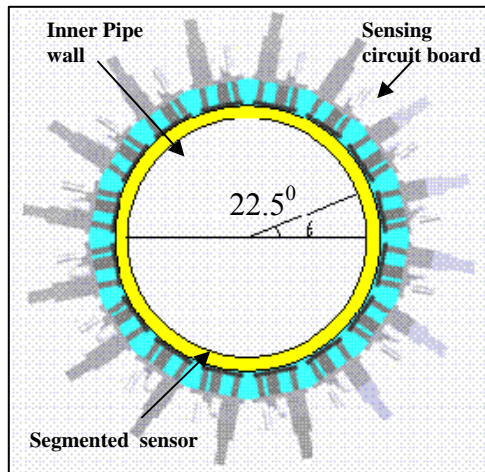
- (a) Choosing the mode in the electrostatics module
- (b) Geometry modeling according to dimension to be simulated
- (c) Generating the mesh
- (d) Set electrical properties in the domains
- (e) Set the boundary conditions

The detail of the physical sensor can be found in Table 1.

**Table 1** Design criteria of ECT

No	Item	Parameter
1	Num of electrode plate	16
2	Electrode length	100 mm
3	Inner pipe diameter	100 mm
4	Outer pipe diameter	110 mm
5	Permittivity of the dielectric	$\epsilon_r=80$ (water) $\epsilon_r=1$ (air) $\epsilon_r=3$ (oil)

Figure 2 shows an arrangement of 16 electrodes sensor on pipelines that has been designed by PROTOM Research Group, UTM, to be mounted on an acrylic pipe with 110 mm in diameter and wall thickness of 0.5 cm,  $R_1$  is inner pipeline radius 5cm ,  $R_2$  is outer pipeline radius, 5.5 cm and electrode stretch angle  $\theta$  is  $22.5^\circ$ .

**Figure 2** Illustration of sixteen sectors of portable ECT

## 2.2 Preparing for Simulations

The modelling approach used in this study can be listed as:

- (1) Choosing the mode in the EM Module
- (2) Drawing the sensor geometries

- (3) Generating the mesh
- (4) Set electrical properties in the domains
- (5) Set the boundary conditions
- (6) Solve and find the field distribution
- (7) Use the post-processing capabilities in COMSOL to compute capacitance and voltage

The 2D and corresponding 3D geometries of the 16 segmented portable ECT are illustrated in Fig. 3. The detail of the sensor can be found in Table 1.1.

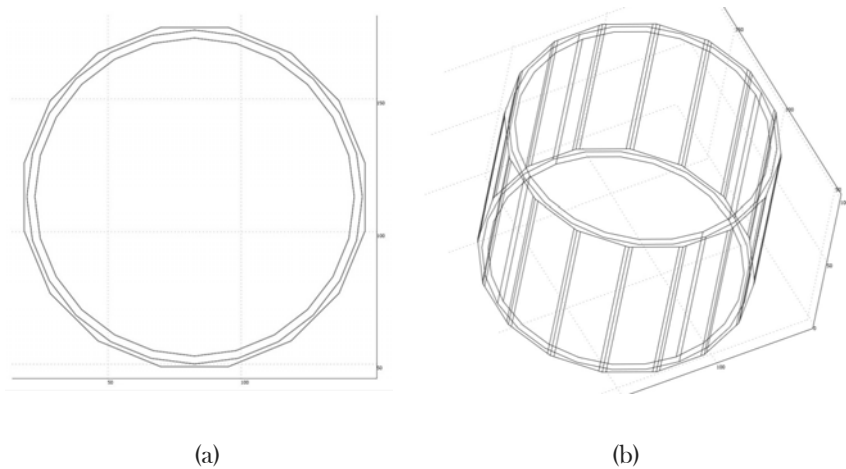


**Figure 3** a) 2D segmented geometry of portable ECT sensor, b) 3D geometry of portable ECT sensor

### 2.3 FEM Meshing

In this work, besides the insulating pipe, measurement electrodes, guard electrodes, the geometry includes the spatial discretization of the inner part of the sensor, a  $32 \times 32$  square matrix has a number of 1024 pixels but only 830 pixels contribute to represent the image plane and another 194 pixels lie outside the pipe boundary. This diagram corresponds to the space within the  $R_i$  radius in Fig.2.

The meshes used to apply the FEM scheme. Figure 4 shows the finite element meshing in 2D of the portable ECT as appear in COMSOL Multiphysics. The meshing is performed with different parameters for each zone in order to get uniform definition in the area to be visualized and much higher definition near the electrodes, where need more accuracy.

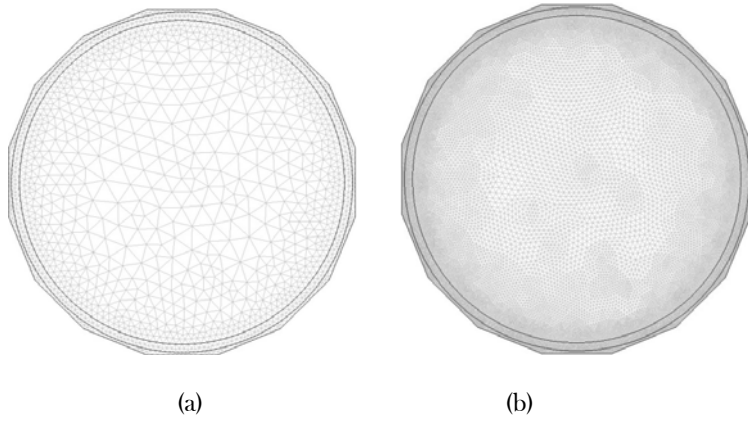


**Figure 4** FEM Meshing; (a) initial mesh, (b) finer mesh

## 2.4 Set Electrical Properties Domain and Boundary Condition

After drawing the geometry of ECT, the next step is to assign the boundary and subdomain settings. Boundary conditions used are ground, port and distributed capacitance. On the other hand, the conditions for subdomain depend on the constant permittivity such as water, air and oil. The equations used for the boundary and subdomain conditions as follows;

- 1)  $n(D_1 - D_2) = \frac{\epsilon_0 \epsilon_r (V_{ref} - V)}{d}$ , for distributed Capacitance.
- 2)  $V = 0$  for ground
- 3)  $C = \frac{Q}{V}$ , for port (excitation electrode)

The subdomain setting is;

$$1) -\nabla \cdot d\epsilon_0 \epsilon_r \nabla V = d\rho$$

where;

$\epsilon_0$ , is the relative permittivity

$\rho$ , is the space charge density in  $C/m^3$

$d$ , is the thickness in mm

## 2.5 Preparing of Excitation Electrode

ECT operates by reading the potential difference from the excited electrode to the detecting electrode. For example, when electrode 1 is given voltage, the rest of the electrode will be the detecting electrode, the potential difference between inter-electrode capacitance will verified.

The basic principles of ECT sensors have been described by many publications. In ECT, the object to be imaged is surrounded by electrodes, which act as both sources and detectors. The electrodes are excited one by one, or in pairs depending on the protocol used. At any point in time only one electrode or a pair of electrodes is excited, while the remaining electrodes function as detectors. The term protocol mainly refers to the sequence used to excite the sensor electrodes, and the order in which the signals are acquired.

For example, if electrode 1 is made the source electrode, the rest electrodes function as detector electrodes. The detector electrodes are connected to the virtual ground terminals, so that they remain at zero potential with respect to ground. The capacitances between electrode 1 and the others are measured. After measuring all the possible pairs of capacitances, electrode 2 is made the source electrode and the measurement process is repeated. The whole cycle of exciting an electrode and measuring the resulting inter-electrode capacitances is repeated. The total number of electrode  $s$  given by  $N$  and the independent inter-electrode capacitance measurements  $M$  is given by;

$$M = \frac{N(N-1)}{2} \quad (2)$$

Figure 5 showing a schematic representation of electric field lines that exist between any two electrodes are not straight. The field lines are curved instead.

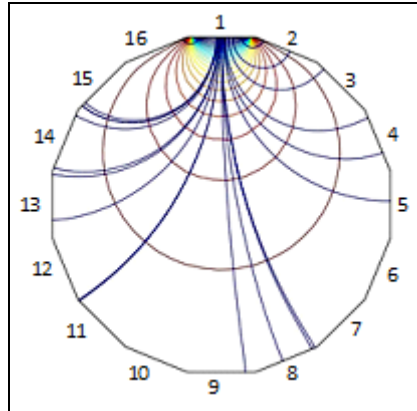


**Figure 5** Number of electrodes on ECT

### 3.0 ELECTRICAL POTENTIAL DISTRIBUTION

It is difficult to calculate an inter-electrode capacitance which relate with the relative permittivity distribution  $\varepsilon(r)$  and potential distribution  $\phi(r)$ , by using the Laplace equation is still too difficult to solve for the geometry and the boundary conditions, thus a finite element method (FEM) software simulation package is need to be used to find the electric field distributions. In this project the COMSOL Multiphysic is used to carry out the FEM simulation to find the electrical potential distribution in the space of the sensor.

Therefore we can relate the permittivity and potential difference in (1) as follows (3) to be (4);

$$C = \frac{kA\varepsilon_o}{d} \quad (3)$$

Where;

$C$  = capacitance (F)

$\varepsilon_o$  = permittivity of dielectric (fluid flow)

$k$  = the constant

$A$  = area of the plate

$d$  = the distance between those plates



$$C = \frac{Q}{V_{1,2}} \quad (4)$$

Where;

$Q$  is the charge of the two conductors

$V_{1,2}$  is the voltage difference between the two conductors

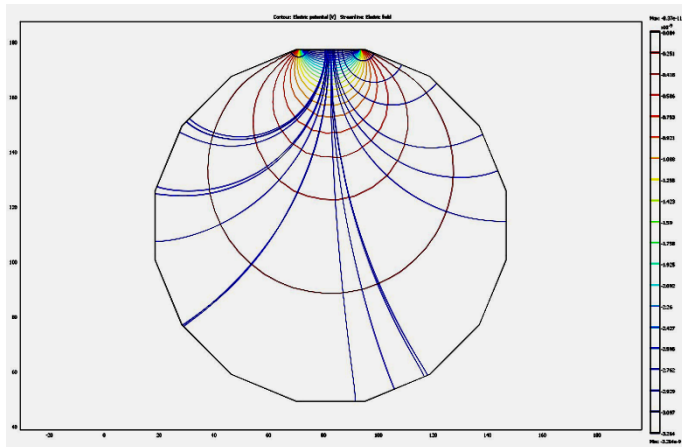
Note that the Equation (3) and (4) can be used to measure the capacitance of a certain material flow in a pipeline.

### 3.1 Electrical Potential Distribution

For the Electrical potential distribution as in (5), the Electrostatic solver is used, at it has after we set the boundary condition and subdomain setup, as it has better performance for solving such as Laplace and Poisson.

$$\nabla \cdot [\varepsilon(r) \nabla \varphi(r)] = 0 \quad (5)$$

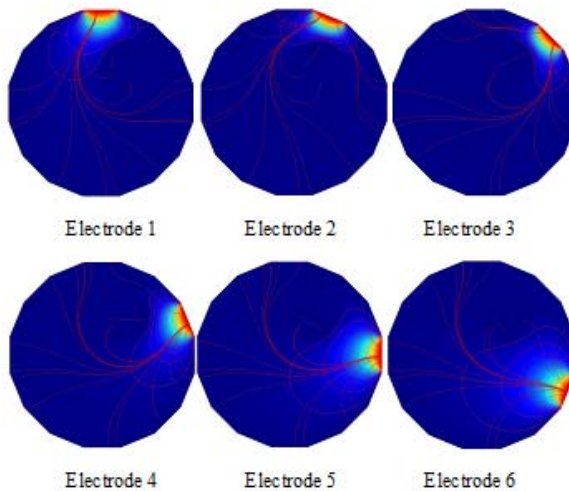
Finally, capacitance calculation is performed between the model electrode-pairs by means of the method describe in section 2.0. Figure 5 shows the electrical field lines distribution when electrode 1 is charged (excitation electrode), in that moment measurements (simulated) are taken between it and the other 15 electrodes (grounded electrodes). The same occurs with all electrodes to make a total,  $M= 120$  measurements.



**Figure 5** Electrical field and potential lines for single excited electrode

### 3.2 Single Excitation Electrode for 16 Sensor

To verify simulation, an annular phantom was created. The phantom used in this case is as illustrated in 2D case, where a 20 mm in diameter is located with its right at coordinates  $x=60$  mm and  $y=125$  mm. The permittivity distribution in this case is water, with relative permittivity  $\epsilon_r=80$ . The electrical field distribution for 2D simulation, when electrode 1 is excited is illustrated in Fig. 6.



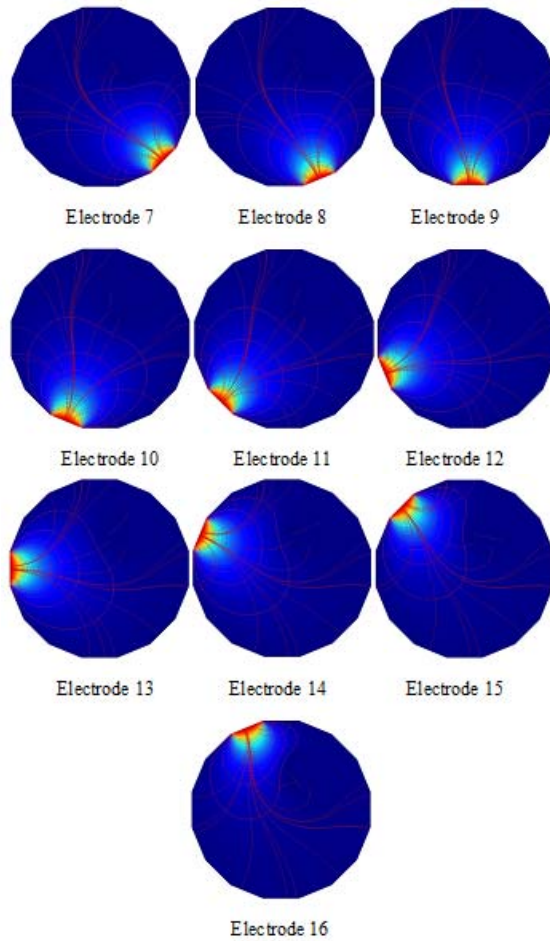


**Figure 6** Potential distribution and image reconstructed

#### 4.0 RESULT SIMULATION

The simulation was verified as followed:

- I. image reconstructed for 2D when electrode 1 is excited.
- II. electrical field lines for 3D simulation when electrode 1 is excited.
- III. image reconstructed for 2D when all electrode is excited
- IV. image reconstructed simulation with different mixture of permittivity

#### 4.1 Standing Capacitance Measurement

Capacitance is performed between the model electrode-pairs and the electrical field distribution for 2D and 3D simulation, when electrode 1 is excited, are illustrated in Fig.7, and all electrode excited in Fig. 8. The phantom used as illustrated in the 2D where a 50 mm in diameter, cylindrical phantom of water surrounded by air, is located with its centre at coordinates  $x=70$  and  $y=130$ . As can be seen, the electrical field lines are deflected, depending on material distribution.

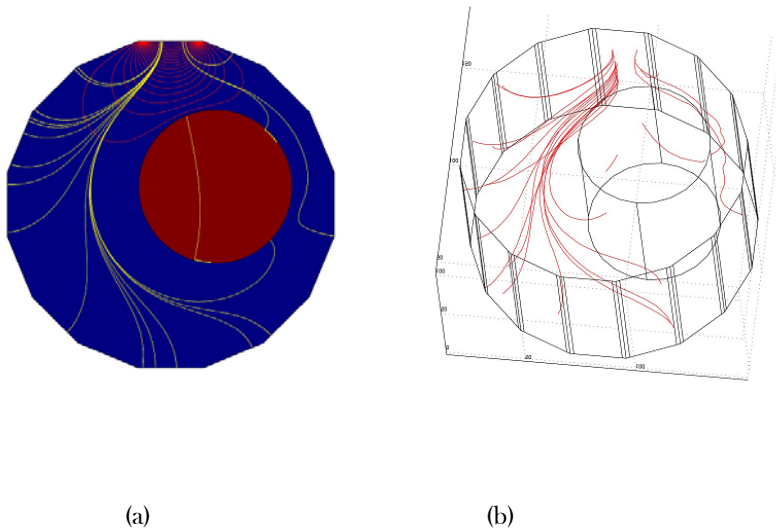


**Figure 7** Results from (a) 2D and (b) 3D simulation, respectively. Blue area is sensing region represent air ( $\epsilon_{\text{air}}=1$ ), and red area represents water ( $\epsilon_{\text{water}}=80$ )

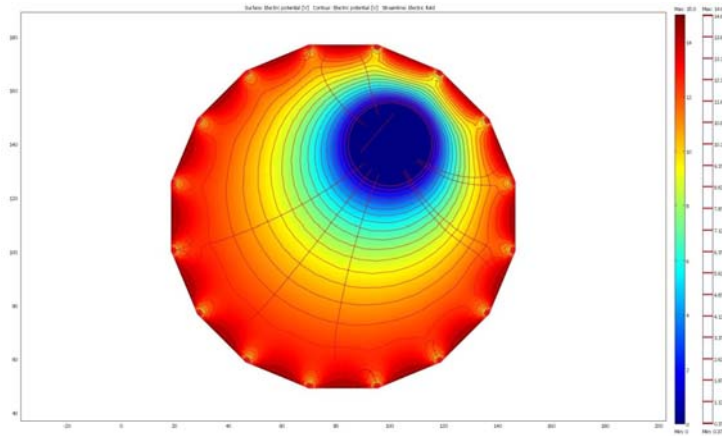
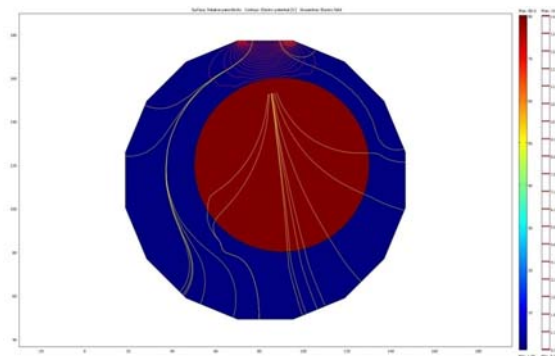


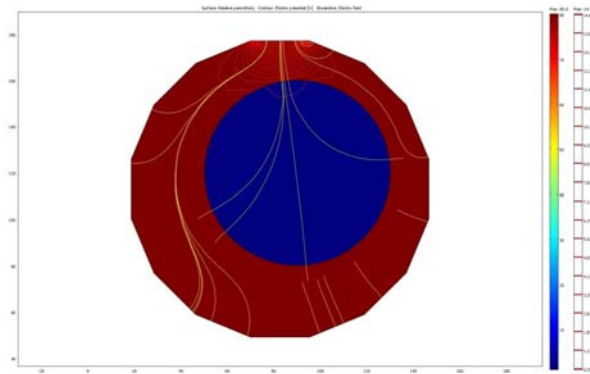
**Figure 8** Electrical field distribution for 2D when all electrodes was excited

#### 4.2 Different Mixture of Permittivity

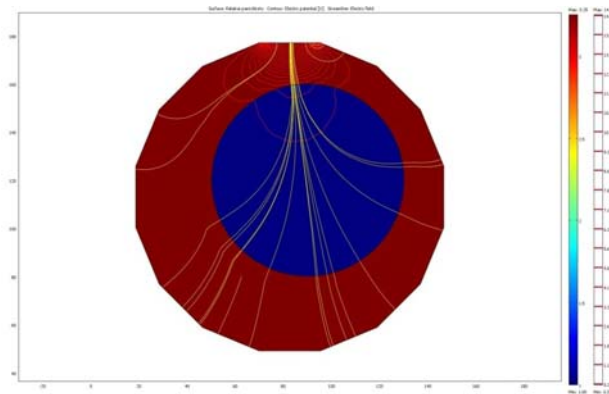
Figure 9 below shows that the degree of penetration of electrical field depends on the permittivity of the material. We know that  $\epsilon_{\text{water}}$  is 80,  $\epsilon_{\text{air}}$  is 1 and  $\epsilon_{\text{oil}}$  is 3.25, thus water has the highest permittivity and air has the lowest permittivity. When the permittivity is water, the electrical field seem to be reflected more than the oil or air. This is due to the permittivity of the phantom, as the permittivity increases the degree of reflected electrical field will also increase. In addition, the electrical field lines also tend to bend more around the phantom as the permittivity of the phantom gets higher because of the increasing of conductivity.



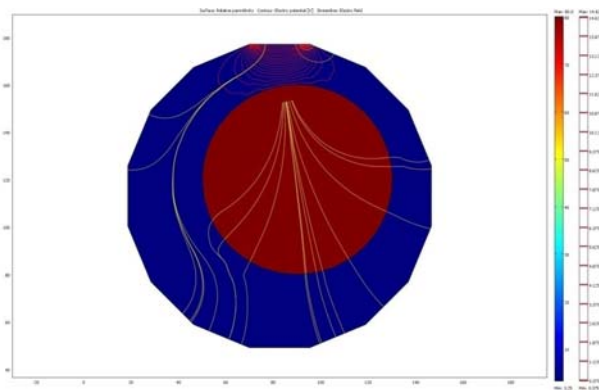
**(a)** Electrical field lines of air (blue) and water (red)



(b) Electrical field lines of water (red) and air (blue)



(c) Electrical field lines of oil (red) and air (blue)



(d) Electrical field lines of oil (blue) and water (red)

**Figure 9** Degree of penetration of electrical field depends on the permittivity of the material (a)-(d)

## 5.0 CONCLUSIONS

The image reconstructed 16 electrode was successfully simulated by using COMSOL Multiphysic. According to the simulation results of fan beam 16 electrodes, the electrical properties such as potential difference, electrical field lines, potential lines, capacitance in ECT, and permittivity of the dielectric can be verified. The 2D and 3D geometries of ECT sensors was successful generated.

## ACKNOWLEDGEMENTS

The authors would like to thank the following individual and organization: Research University Grant of Universiti Teknologi Malaysia (Grant No. QJ130000.7123.00J04) and Science Fund of Ministry of Science, Technology & Innovation, Malaysia (Grant No. 03-01-06-SF0193; Vot 79128).

## REFERENCES

- [1] Huang, M., Liu, C. and Shen, L. C. 1995. Monitoring the Contamination of Soils by Measuring Their Conductivity in the Laboratory Using a Contactless Probe. *Geophysical Prospecting*. 43: 759-778.
- [2] Martinez Olmos, M. A Carvajal *et al.* 2008. Development of an Electrical Capacitance Tomography System using Four Rotating Electrodes.
- [3] Ruzairi Abdul Rahim. 2008. High Speed Data Acquisition System for Computer Tomographic Imaging Instrumentation. Universiti Teknologi Malaysia.
- [4] Warsito Warsito *et al.* 2007. Electrical Capacitance Volume Tomography. *IEEE Sensors Journal*. 7: 4.
- [5] Hafizah Talib, Junita Mohamad Saleh and Zalina Abdul Aziz. 2009. Flow Process Identification from Electrical Capacitance Tomography Data Using Ensemble of Multilayer Perceptrons. School of Electrical and Electronics Engineering Campus, Universiti Sains Malaysia.
- [6] Noberto Flores, J. Carlos Gamio, Carlos Ortiz\_Aleman and Enrique Damian. 2005. Sensor Modeling for an Electrical Capacitance Tomograpgy System Applied to Oil Industry. Proceeding of the COMSOL Multiphysocs User's Conference, Boston.
- [7] Kjell Joar Alme and Saba Mylvaganam. 2006. Analyzing 3D and Conductivity Effects in Electrical Tomography System Using COMSOL Multiphysics EM Module. Proceedings of the Nordic COMSOL Conference.